Langmuir

Letter

pubs.acs.org/Langmuir

Deactivation of Microbubble Nucleation Sites by Alcohol–Water Exchange

Xuehua Zhang,*[,†,‡] Henri Lhuissier,[‡] Oscar R. Enríquez,[‡] Chao Sun,[‡] and Detlef Lohse*[,‡]

[†]Department of Chemical and Biomolecular Engineering and Particulate Fluid Processing Center, University of Melbourne, Parkville, VIC 3010, Australia

[‡]Department of Science and Technology, J. M. Burgers Center for Fluid Dynamics and Mesa+, University of Twente, P.O. Box 217, 7500 AE Enschede, The Netherlands

Supporting Information

ABSTRACT: The ethanol–water exchange process is one of the standard methods of generating nanobubbles at a solid–water interface. In this work, we examine whether the nanobubbles formed by the solvent exchange can initiate microbubble formation as the temperature increases, thus acting as nuclei. This, however, is not the case: the nanobubbles are stable and do not facilitate microbubble formation. Instead, the process of solvent exchange, which aids the formation of nanobubbles and even microbubbles on some hydrophobic substrates under ambient conditions, suppresses microbubble nucleation on graphite and hydrophilic micropit-decorated substrates at high temperature (i.e., deactivates the nucleation sites for microbubble formation). We ascribe this behavior to the prewetting of the surface by the alcohol and the stability of the nanobubbles to the temperature increase. The findings in this study have implications for the prevention of bubble formation for a range of applications.

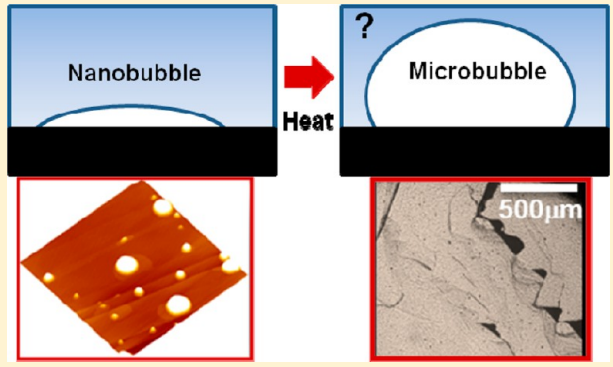

INTRODUCTION

The "inverse" of water droplets on surfaces in air is air bubbles on surfaces in water. Just as droplets, they come in various sizes. What is currently intriguing in the field of colloid and surface science is surface nanobubbles (i.e., gaseous domains of nanoscale thickness).[1−3] These nanobubbles exist on hydrophobic surfaces in contact with water and render the already complicated hydrophobic–water interfaces even more elusive. It has been reported that the presence of nanobubbles can influence a range of interfacial behaviors, such as thin liquid film rupture,[4] hydrodynamic boundary conditions,[5] particle or molecular adsorption,[6] and surface corrosion and catalysis processes.[7] Research efforts in the past decade have revealed that the formation of nanobubbles is closely related to the surface history. For example, a temperature gradient, electro- or photochemical reactions, or pressure fluctuations in the system can all induce nanobubbles. One of the most often used methods of producing nanobubbles is the solvent-exchange process[8] where a hydrophobic substrate is first exposed to a short-chain alcohol, such as ethanol or propanol, and then to water. Given that gases have a higher solubility in alcohol than in water, local gas supersaturation is created during the solvent exchange and nanobubbles form on the interface.[8]

Although counterintuitive, once formed, the nanobubbles are very stable. Under ambient conditions, they can live for several days.[9] Several hypotheses have been proposed to explain the long life of surface nanobubbles, including a contamination shell on the bubble surface,[10] dynamic equilibrium theory,[11] and coexisting gas layers.[12,13] Recently, three research groups have independently proposed the important role of pinning at the three-phase boundary of nanobubbles and the gas saturation level in the liquid phase.[14−16] Nanobubbles also demonstrate strong stability under long, gentle sonication[17] and under a massive pressure reduction through a rarefaction wave.[18]

In this Letter, we wonder how the formation process and the presence of surface nanobubbles influence microbubble nucleation with increasing temperature. Such a study may (i) shed light on the relation between nanobubbles and normal microbubbles from cavitation and (ii) provide a potential method of controlling microbubble nucleation in some practical processes. According to nucleation theory, the onset of bubble nucleation in a stationary system can be facilitated by micro/nanoscale physical or chemical features on the substrate.[19−25] In particular, the presence of tiny gas pockets trapped inside the crevices on the surface, called Harvey nucleation sites,[24] has been used to rationalize the nucleation of bubbles, either under pressure reduction or under boiling conditions. Bremond et al.[26] have demonstrated that the bubbles specifically form on the built-in micropits on a flat background under pressure

Received: May 25, 2013
Revised: July 26, 2013
Published: July 26, 2013

   dx.doi.org/10.1021/la402015q | Langmuir 2013, 29, 9979−9984

reduction. Later, Borkent et al. showed that the cavitation threshold can be quantitatively predicted, in perfect agreement with the experimental findings.[27] However, in another paper Borkent et al. have shown that even under a massive pressure reduction down to −60 bar surface nanobubbles do not act as nuclei for microbubble formation.[18]

The question to be addressed here is whether surface nanobubbles act as nucleation sites with increasing temperature and thus initiate the onset of microbble formation. We find that surface nanobubbles do not facilitate the initiation of microbubbles at high temperatures. Instead, the very same solvent-exchange process, which aids the formation of nanobubbles and even microbubbles on some hydrophobic substrates, can suppress the onset of bubble nucleation.

EXPERIMENTAL SECTION

The substrates used in this work are summarized in Table 1. Type I is a planar substrate composed of freshly cleaved, highly oriented pyrolytic graphite (HOPG). We fabricate micropits on silicon wafers using soft lithography and reactive-ion etching techniques in a clean room. With this procedure, we made pits with a minimum diameter of a couple of micrometers and a depth of tens of micrometers (type II). To guarantee that air is trapped inside such cavities upon immersion in water, we made the pit superhydrophobic by creating a black silicon structure on the bottom[28] and then applied an octafluorocyclobutane (C4F8) coating (type III).

Table 1. Substrates for Bubble Formation

	type I (HOPG)	type II (uncoated)	type III (coated)
micropit size	N/A	40 μm, 50 μm, 100 μm	10 μm, 50 μm
advancing and receding water angles	90 ± 5, 66 ± 3	62 ± 1, 47 ± 1	152 ± 1, 17 ± 1
after the exchange at 22 °C	nanobubbles	no microbubbles	microbubbles

Water was prepared with a Milli-Q system and kept for at least 12 h at 4 °C to equilibrate with air before use. The ethanol was freshly distilled. When degassed ethanol or water was used, the liquids were stirred and stored under a reduced pressure of 80 kPa until no bubbles formed. During the standard solvent-exchange process, the substrate was first exposed to ethanol, and then the ethanol was exchanged with a large amount of water. The nanobubbles were imaged by tapping mode AFM on HOPG after the exchange, following the protocol in our previous work.[29,30] We used the setup as shown in the schematic drawing in Supporting Information to observe the formation of the microbubbles. The temperature of the heater was set at 85 °C, and the substrate was placed on a hot block and then heated from 22 °C until microbubbles were observed under the optical microscope.

RESULTS AND DISCUSSION

On a Planar Substrate: Highly Orientated Pyrolytic Graphite. Figure 1 shows the microbubble formation on the HOPG surface with the increase in the temperature. When HOPG was directly exposed to air-equilibrated water (no nanobubbles form in this case) and then heated to 85 °C, bubbles were observed along the cleavage steps with a typical number density of 5 to 80 microbubbles over an area of 2 mm^2 as shown in Figure 1A. After the solvent-exchange process was performed by first using air-saturated ethanol and then water to produce nanobubbles on the surface, only 0 to 1 microbubble formed after the temperature of the HOPG had been increased to 95 °C (where even more microbubbles should form than at 85 °C), as shown in Figure 1B. To confirm that the solvent-exchange process did not alter the substrate permanently, the water together with nanobubbles was removed by exposing the HOPG surface to air. Therefore, the substrate was reset to the state prior to the solvent exchange. When the substrate was then heated a second time in air-equilibrated water, many microbubbles formed again at 85 °C as shown in Figure 1C.

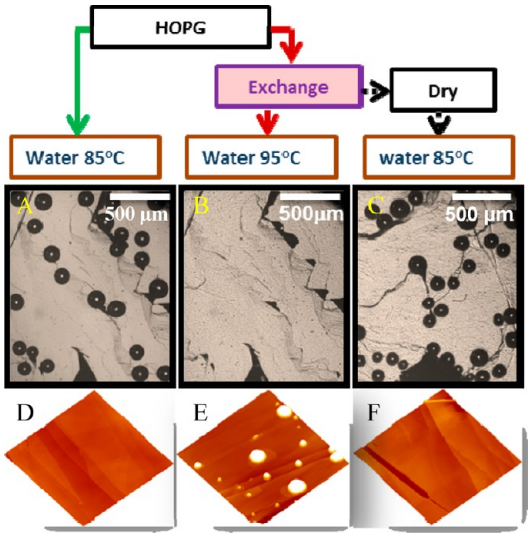

Figure 1. Microbubbles nucleated on highly oriented pyrolytic graphite (HOPG) at elevated temperature. (A) Microbubbles formed on HOPG directly exposed to water at 85 °C. (B) After solvent exchange, no microbubbles formed on HOPG at 95 °C. (C) Microbubbles formed again when HOPG was dried after the solvent-exchange process and exposed to water at 85 °C. (D−F) AFM images of HOPG under the same conditions as in A−C, now at room temperature. The area of the AFM images is 5 μm × 5 μm.

We further examined whether nanoscale gaseous domains (nanobubbles or micropancakes) remained on the surface after exposure to a high temperature. On the HOPG surface, nanobubbles and micropancakes were produced by solvent exchange and imaged by AFM under ambient conditions. Then the temperature of the HOPG was increased to ∼80 °C and then cooled to room temperature for AFM imaging. It was found that both nanobubbles and micropancakes (Figure 2A,B) remained on the surface after exposure to ∼80 °C in Figure 2C,D. The surface coverage of the nanobubbles and micropancakes changed from 54 to 65%, and the number density of nanobubbles remained almost the same (∼60−64 over 100 μm^2). This result demonstrates that nanobubbles remain stable with the increase in temperature and do not evolve into macroscopic bubbles. The mechanism behind such stability may be related to the strong pinning at the three-phase boundary, which needs to be confirmed by more quantitative experimental studies in the future. We did not manage to obtain AFM images of the nanobubbles at 80 °C as a result of the thermal drift of our instruments. Thus we do not know whether the morphology or size of the nanobubbles transiently changes at such high temperature.

There are three possible reasons that microbubbles do not form after the solvent exchange: (i) Nucleation sites are prewetted by the ethanol during the solvent-exchange process. (ii) On an untreated substrate, microbubbles nucleate at the intrinsic nucleation sites (i.e., imperfections) on the substrate with increasing temperature. After the solvent exchange, such intrinsic sites may be buried under the nanobubbles that isolate the sites from the liquid phase. Whether microbubbles form at

dx.doi.org/10.1021/la402015q | Langmuir 2013, 29, 9979−9984

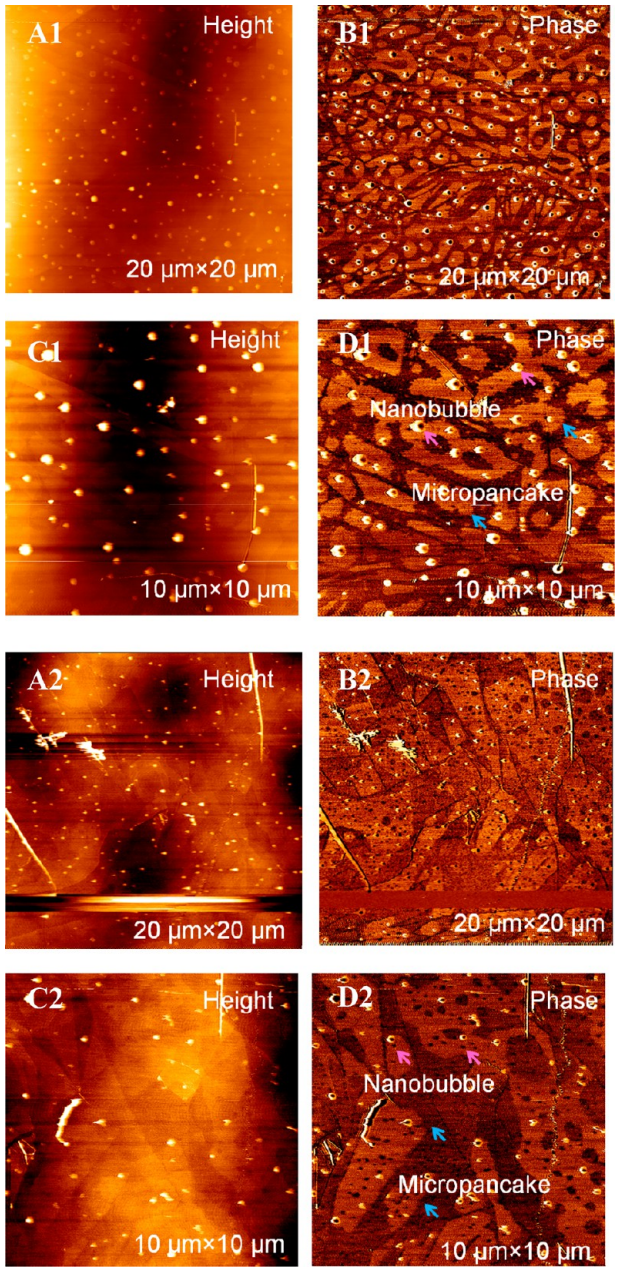

Figure 2. AFM images of nanobubbles and micropancakes on the HOPG surface. (A1–D1) in water at 22 °C. The scan sizes are (A, B) 20 μm × 20 μm and (C, D) 10 μm × 10 μm. (A2–D2) In water after heating to 80 °C and then cooling to 22 °C. The pink arrows point to two nanobubbles, and the blue arrows point to two micropancakes in D1 and D2, two different imaging areas. Both nanobubbles and micropancakes remain on the surface after heating.

higher temperature is determined by the stability of nanobubbles at this temperature, not by the activity of the intrinsic nucleation sites on the substrates. (iii) The nanoscale gaseous layer (i.e., nanobubbles and micropancakes) acts as an insulating layer, preventing heat transfer. In cases ii and iii, the preformation of nanobubbles is required for the deactivation of microbubbles. Explanation iii can be immediately ruled out, given that the nanobubble distribution can be sparse and the micropancakes of condensated gas are too thin.

To determine remaining possibilities i and ii, we have performed the solvent-exchange process by using degassed ethanol and degassed water and have further exchanged the degassed water with air-equilibrated water. By this process, the substrate was exposed to three solvents: degassed ethanol, degassed water, and air-equilibrated water. The results in Figure 3 show that the exchange of degassed ethanol and degassed

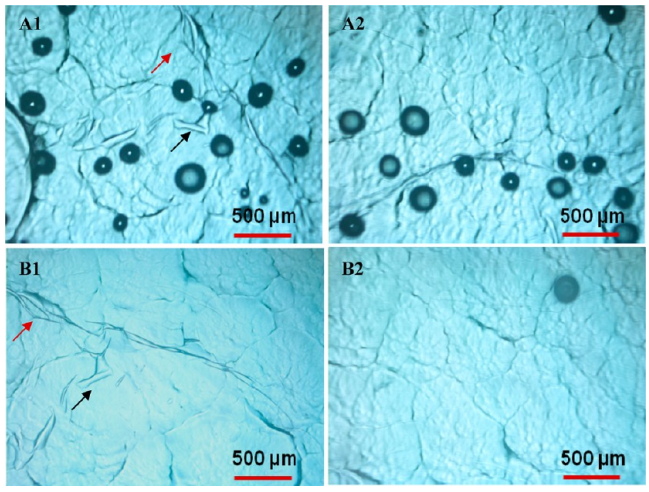

Figure 3. Optical images of HOPG substrate at 85 °C with and without solvent exchange with degassed ethanol and water. (A1, A2) Direct exposure to air-equilibrated water. (B1, B2) In air-equilibrated water after the exchange of degassed ethanol for degassed water. The arrows of the same color in A1 point to the same features on the substrate in B1.

water, which could suppress the nucleation of microbubbles equally well: no microbubbles formed at 85 °C. Therefore, the presence of surface nanobubbles resulting from the solvent-exchange process was not critical to the deactivation of the microbubble nucleation. The prewetting by the degassed alcohol itself was sufficient to deactivate the microbubble nucleation. However, in the case in which deactivation was achieved by the exchange of air-equilibrated solvents, it is critical that the nanobubbles produced by this process were stable at increasing temperature. Otherwise, they could evolve into microbubbles. Therefore, reasons i and ii could both play important roles in the deactivation by solvent exchange.

In the experiments, when isopropanol was used instead of ethanol during the solvent-exchange process, we obtained similar results: the nucleation of microbubbles could be deactivated by the exchange of isopropanol for water. In previous work, nanobubbles were also produced by using other short-chained alcohols such as methanol or propanols.[19] They are all miscible with water and can wet the HOPG surface. We also examined the stability of nanobubbles on other types of substrates: silicon coated with octadecyltricholorosilane (OTS) with a contact angle of 110° for water or coated with 1*H*,1*H*,2*H*,2*H*-perfluorodecyltriethoxysilane (PFDTS) with a contact angle of 120°. Also for these substrates the nanobubbles remained stable at temperatures close to the boiling point of water.

On Surfaces with Micropits. Substrates with micropits have been used to study the nucleation and growth of bubbles because the micropits can provide well-defined nucleation sites for the bubbles. Here, on the substrates without a hydrophobic coating (type II in Table 1), the contact angle of water was 62°. We compared the temperature for microbubble formation with and without the solvent-exchange process in Figure 4. The micropits with a diameter of 40 μm actively nucleated

dx.doi.org/10.1021/la402015q | *Langmuir* 2013, 29, 9979–9984

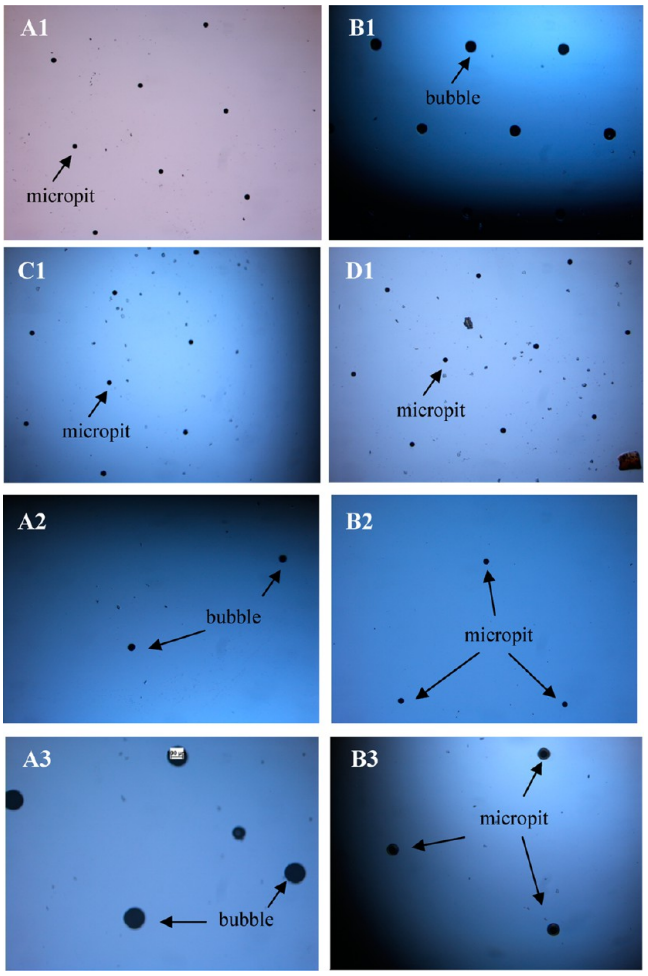

Figure 4. Optical images of the substrates in water. (A1–D1) On 40 μm micropits (type II). (A1) In air. (B1) In air-equilibrated water at 45 °C. (C1) In air-equilibrated water after the solvent exchange at 45 °C. (D1) In air-equilibrated water after the solvent exchange by using degassed ethanol and degassed water at 45 °C. Although some dust particles are visible on C1 and D1, it is clear that no microbubbles formed in C1 and D1. (A2, B2) On 50 μm uncoated micropits (type II). (A1) In air-equilibrated water at 45 °C. (B) In air-equilibrated water after the solvent exchange at 50 °C. (A3–B3) On 100 μm uncoated micropits (type III). (A3) In air-equilibrated water at 50 °C. (B3) In air-equilibrated water after the solvent exchange at 60 °C.

microbubbles at 45 °C under standard conditions (i.e., directly exposed to water). However, after the solvent-exchange process was performed on the substrate, none of the micropits nucleated microbubbles even at 50 °C. If both ethanol and water were degassed before the solvent exchange to prevent the occurrence of surface nanobubbles during this process, no microbubbles formed in the subsequent air-equilibrated water even at 65 °C. Similar results were obtained on the substrate patterned with uncoated micropits with diameters of 50 and 100 μm: microbubbles nucleated in the air-equilibrated water at 45 and 50 °C, respectively. Again, after the solvent-exchange process, no microbubbles formed on the micropits at the same or even higher temperature.

We could not examine by AFM whether nanobubbles were produced inside the micropits by the solvent-exchange process. However, from previous work[29] we know that it is difficult to produce nanobubbles on a noncrystalline substrate with similar hydrophobicity, for example, glassy carbon or trimethylchlorosilane-coated silicon. Here, the microbubble deactivation on micropits can presumably be attributed to reason i above (i.e., prewetting by the alcohol).

We note that the deactivation by solvent exchange is most effective at slow heating rates. The above results were obtained when the copper block and the substrate (as shown in the schematic drawing in Supporting Information) were warmed from room temperature (22 °C) until microbubbles formed with the maximum temperature set at 80 °C. If the copper block was preheated to 60 °C and then the substrate was placed on top, then microbubbles would nucleate on all of the hydrophilic micropits, no matter whether solvent exchange was performed or not. This indicates that the deactivation of the nucleation sites was relative to the gas saturation level in the system. It became ineffective at a high gas saturation level when the system was far from equilibrium during the rapid temperature rise.

On the C4F8-coated substrate (type III) with micropits with diameters of 10 and 50 μm, the contact angle of water was 152°. We found that the solvent-exchange process could already produce microbubbles following the pattern of the micropits even under ambient conditions as shown in Figure 5. Those microbubbles were not uniform with the diameter ranging from 0 to 250 μm, indicating the heterogeneity in the gas saturation level during solvent mixing. Upon the increase in temperature to 85 °C, those microbubbles became larger as shown in Figure 5C1. In our previous work, we observed that some microbubbles with a lateral diameter of up to 10 μm and several hundreds of nanometers in height could be produced simultaneously with nanobubbles by the solvent-exchange process on planar hydrophobic substrates, such as the OTS-Si substrate.[30] With the increase in temperature close to the boiling point, these microbubbles on a planar substrate did not grow substantially, as far as we could judge within the optical resolution. It will be interesting to discover whether the growth of the microbubbles in Figure 5C1 is related to the micropit structure of the substrate underneath. In other words, the nanobubble stability with respect to increasing temperature might be exclusive for microbubbles sitting on a flat substrate.

■ CONCLUSIONS

Surface nanobubbles are stable and do not initiate the formation of microbubbles with increasing temperature. The solvent-exchange process, which produces nanobubbles or even microbubbles under ambient conditions, can deactivate the bubble nucleation sites and lead to a higher temperature for the formation of bubbles on both HOPG and hydrophilic micropits at low heating rates. We attributed the effect of the solvent exchange on microbubble formation to the prewetting of the substrates by the alcohol, and the stability of the nanobubbles to increasing temperature.

■ OUTLOOK

The findings in this Letter may have implications in the prevention of microbubble formation in applications. The deactivation of the nucleation sites can be achieved by the solvent-exchange process based on the prewetting of many substrates of moderate hydrophobicity. In practice, we may apply a thin layer of alcohol to a substrate and then immediately expose it to water to deactivate the nucleation sites. This process does not need an expensive setup or high

dx.doi.org/10.1021/la402015q | *Langmuir* 2013, 29, 9979–9984

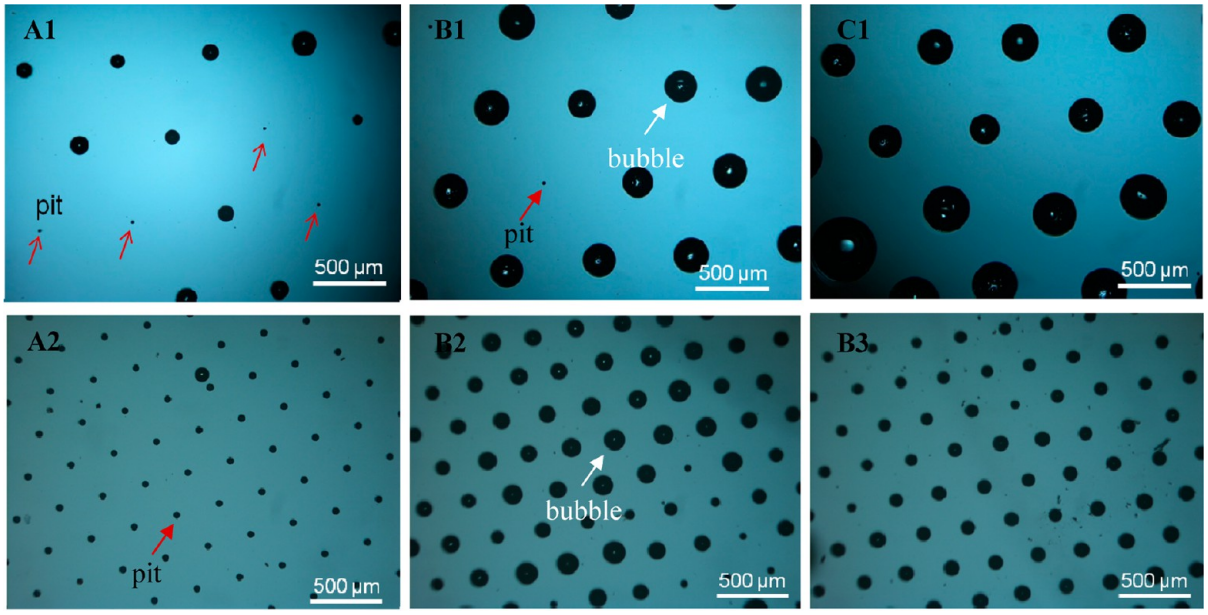

Figure 5. Optical images of the substrate patterned with C4F8-coated 10 and 50 μm micropits (type III). (A1) During the solvent exchange at 10% ethanol under ambient condition. (B1) In air-equilibrated water under ambient conditions after the solvent exchange. (C1) At 85 °C. Microbubbles form during the exchange, and their size is not uniform during the solvent exchange as a result of the flow pattern. All of the microbubbles produced by the solvent exchange became larger with increasing temperature. (A2) C4F8-coated 10 and 50 μm micropits. (B2, B3) Two areas in air-equilibrated water under ambient conditions after the solvent exchange. The bubble size was not uniform due to the heterogeneous gas saturation generated during the solvent exchange.

energy consumption to degas the system but can effectively alleviate the damage caused by unwanted cavitation.

■ ASSOCIATED CONTENT

Supporting Information

Schematic drawing of the setup for bubble formation with increasing temperature. This material is available free of charge via the Internet at http://pubs.acs.org

■ AUTHOR INFORMATION

Corresponding Author

*E-mail: xuehuaz@unimelb.edu.au; d.lohse@utwente.nl.

Notes

The authors declare no competing financial interest.

■ ACKNOWLEDGMENTS

We gratefully acknowledge Professor Andrea Prosperetti for inspiring discussions. X.Z. acknowledges support from the Australian Research Council (FFT120100473). This work is part of the research programme of the Foundation for Fundamental Research on Matter (FOM), which is part of The Netherlands Organisation for Scientific Research (NWO), and it has been supported by an ERC Advanced Grant.

■ REFERENCES

(1) Hampton, M. A.; Nguyen, A. V. Nanobubbles and the Nanobubble Bridging Capillary Force. *Adv. Colloid Interface Sci.* **2010**, *154*, 30−55.
(2) Seddon, J. R. T.; Lohse, D. Nanobubbles and Micropancakes: Gaseous Domains on Immersed Substrates. *J. Phys.: Condens. Matter* **2011**, *23*, 133001.
(3) Craig, V. S. J. Very Small Bubbles at Surfaces-The Nanobubble Puzzle. *Soft Matter* **2011**, *7*, 40−48.
(4) Stockelhuber, K.; Radoev, B.; Wenger, A.; Schulze, H. Rupture of Wetting Films Caused by Nanobubbles. *Langmuir* **2004**, *20*, 164−168.
(5) Finger, A.; Johannsmann, D. Hemispherical Nanobubbles Reduce Interfacial Slippage in Simple Liquids. *Phys. Chem. Chem. Phys.* **2011**, *13*, 18015−18022.
(6) Wu, Z. H.; Zhang, X. H.; Zhang, X. D.; Gang, L.; Sun, J. L.; Zhang, Y.; Li, M. Q.; Hu, J. Nanobubbles Influence on BSA Adsorption on Mica Surface. *Surf. Interface Anal.* **2005**, *37*, 797−801.
(7) Belova, V.; Gorin, D. A.; Shchukin, D. G.; Mohwald, H. Selective Ultrasonic Cavitation on Patterned Hydrophobic Surfaces. *Angew. Chem., Int. Ed.* **2010**, *49*, 7129−7133.
(8) Zhang, X. H.; Zhang, X. D.; Lou, S. T.; Zhang, Z. X.; Sun, J. L.; Hu, J. Degassing and Temperature Effects on the Formation of Nanobubbles at the Mica/Water Interface. *Langmuir* **2004**, *20*, 3813−3815.
(9) Zhang, X. H.; Quinn, A.; Ducker, W. A. Nanobubbles at the Interface between Water and a Hydrophobic Solid. *Langmuir* **2008**, *24*, 4756−4764.
(10) Ducker, W. A. Contact Angle and Stability of Interfacial Nanobubbles. *Langmuir* **2009**, *25*, 8907−8910.
(11) Brenner, M. P.; Lohse, D. Dynamic Equilibrium Mechanism for Surface Nanobubble Stabilization. *Phys. Rev. Lett.* **2008**, *101*, 21.
(12) Dammer, S. M.; Lohse, D. Gas Enrichment at Liquid-Wall Interfaces. *Phys. Rev. Lett.* **2006**, *96*, No. 206101.
(13) Peng, H.; Hampton, M.; Nguyen, A. Nanobubbles Do Not Sit Alone at the Solid−Liquid Interface. *Langmuir* **2013**, *29*, 6123−6130.
(14) Zhang, X. H.; Chan, D. Y. C.; Wang, D. Y.; Maeda, N. Stability of Interfacial Nanobubbles. *Langmuir* **2013**, *29*, 1017−1023.
(15) Weijs, J. H.; Lohse, D. Why Surface Nanobubbles Live for Hours. *Phys. Rev. Lett.* **2013**, *110*.
(16) Liu, Y. W.; Zhang, X. R. Nanobubble Stability Induced by Contact Line Pinning. *J. Chem. Phys.* **2013**, *138*, 6.
(17) Brotchie, A.; Zhang, X. H. Response of Interfacial Nanobubbles to Ultrasound Irradiation. *Soft Matter* **2011**, *7*, 265−269.
(18) Borkent, B. M.; Dammer, S. M.; Schonherr, H.; Vancso, G. J.; Lohse, D. Superstability of Surface Nanobubbles. *Phys. Rev. Lett.* **2007**, *98*, 204502.
(19) Bourdon, B.; Rioboo, R.; Marengo, M.; Gosselin, E.; De Coninck, J. Influence of the Wettability on the Boiling Onset. *Langmuir* **2012**, *28*, 1618−1624.

(20) Thomas, O. C.; Cavicchi, R. E.; Tarlov, M. J. Effect of Surface Wettability on Fast Transient Microboiling Behavior. *Langmuir* **2003**, *19*, 6168−6177.
(21) Jones, S. F.; Evans, G. M.; Galvin, K. P. Bubble Nucleation from Gas Cavities - A Review. *Adv. Colloid Interface Sci.* **1999**, *80*, 27−50.
(22) Caupin, F.; Herbert, E. Cavitation in Water: A Review. *C. R. Phys.* **2006**, *7*, 1000−1017.
(23) Morch, K. A. Reflections on Cavitation Nuclei in Water. *Phys. Fluids* **2007**, *19*, 7.
(24) Harvey, E. N.; Barnes, D. K.; McElroy, W. D.; Whiteley, A. H.; Pease, D. C.; Cooper, K. W. Bubble Formation in Animals I. Physical Factors. *J. Cell. Comp. Physiol.* **1944**, *24*, 1−22.
(25) Atchley, A. A.; Prosperetti, A. The Crevice Model of Bubble Nucleation. *J. Acoust. Soc. Am.* **1989**, *86*, 1065−1084.
(26) Bremond, N.; Arora, M.; Ohl, C. D.; Lohse, D. Controlled Multibubble Surface Cavitation. *Phys. Rev. Lett.* **2006**, *96*, 22.
(27) Borkent, B. M.; Gekle, S.; Prosperetti, A.; Lohse, D. Nucleation Threshold and Deactivation Mechanisms of Nanoscopic Cavitation Nuclei. *Phys. Fluids* **2009**, *21*, 10.
(28) Jansen, H.; Deboer, M.; Legtenberg, R.; Elwenspoek, M. The Black Silicon Method - A Universal Method for Determining the Parameter Setting of a Fluorine-Based Reactive Ion Etcher in Deep Silicon Trench Etching with Profile Control. *J. Micromech. Microeng.* **1995**, *5*, 115−120.
(29) Zhang, X. H.; Maeda, N. Interfacial Gaseous States on Crystalline Surfaces. *J. Phys. Chem. C* **2011**, *115*, 736−743.
(30) Zhang, X. H.; Maeda, N.; Craig, V. S. J. Physical Properties of Nanobubbles on Hydrophobic Surfaces in Water and Aqueous Solutions. *Langmuir* **2006**, *22*, 5025−5035.